AtomicControl:
A Crystallography Simulator

by

Edward S. Barnard

Submitted to the Department of Materials Science and Engineering
in partial fulfillment of the requirements for the degree of

Bachelor of Science in Materials Science and Engineering

at the

MASSACHUSETTS INSTITUTE OF TECHNOLOGY

June 2005

MASSACHUSETTS INSTITUTE OF TECHNOLOGY
JUN 06 2005
LIBRARIES

© Edward S. Barnard, 2005. All rights reserved.

The author hereby grants to MIT permission to reproduce and distribute publicly paper and electronic copies of this thesis document in whole or in part.

Author ....
Department of Materials Science and Engineering
May 20, 2005

Certified by ....
Samuel M. Allen
POSCO Professor of Physical Metallurgy
Thesis Supervisor

Accepted by ....
Donald R. Sadoway
John F. Elliott Professor of Materials Chemistry
Chair of the Undergraduate Committee

ARCHIVES

AtomicControl:
A Crystallography Simulator

by

Edward S. Barnard

Submitted to the Department of Materials Science and Engineering
on May 20, 2005, in partial fulfillment of the
requirements for the degree of
Bachelor of Science in Materials Science and Engineering

Abstract

AtomicControl is a software package designed to aid in the teaching of crystallography and x-ray diffraction concepts to materials science students. It has the capability to create an arbitrary crystal structure based on the user's specification of a space group and atomic coordinates. It also can generate a simulated powder diffractogram based on the user's generated crystal. The program is fully interactive and allows the user to view the effects of changes to lattice and atoms in a 3D visualization of the crystal. AtomicControl's x-ray diffraction patterns have been shown to match well with experimental data, proving the validity of the algorithm.

AtomicControl is available online at http://pruffle.mit.edu/atomiccontrol/

Thesis Supervisor: Samuel M. Allen
Title: POSCO Professor of Physical Metallurgy

Acknowledgments

I would like to thank Elizabeth Hager for her help in writing the initial version of AtomicControl. Marc Richard has also been very helpful in developing the lesson plans that have been included in this document. I would like to thank Prof. W. Craig Carter for inspiring this project and for supervising it through the initial version. Finally, Prof. Samuel Allen has been instrumental in advising me through the completion of the project and the writing of this thesis.

The development of this software was supported in part by the MIT Undergraduate Research Opportunities Program Office, and the MIT Alumni Funds for Teaching and Education Enhancement, supported by the classes of 1951, 1952, and 1972.

Contents

1 Introduction **11**

1.1 Motivation 11

1.2 Overview 12

2 Software Model **13**

3 Space Group Symmetry Builder **15**

3.1 Space group definition 15

3.2 Symmetry operators and their matrix representations 16

3.3 Algorithm for crystal generation 17

3.4 Crystal generation results 18

4 X-ray Diffraction Theory **19**

4.1 The reciprocal lattice 21

4.2 Ewald sphere construction 22

4.3 Structure factor 22

4.4 Atomic scattering factor 23

4.5 Ideal powder pattern 25

5 X-ray Powder Diffraction Pattern Algorithm **29**

5.1 Finding valid scattering vectors 29

5.2 Calculation of structure factors 30

5.3 Converting structure factors to powder pattern 30

5.4 Results of diffraction calculations 31

6 User Interface **33**

6.1 Specifying a space group 33

6.2 Populating the unit cell 34

6.3 Viewing the crystal 34

6.4 Virtual diffractometer 36

6.5 Saving and retrieving data 37

7 Lesson Plans **39**

7.1 Redefining the unit cell 39

7.2 Cu_3Au order-disorder transformation 42

7.3 Cubic-to-tetragonal transition 45

8 Conclusions **49**

List of Figures

2.1 Interaction of Java objects in AtomicControl 14
2.2 XML crystal file format. 14

3.1 Various symmetry operators represented as vector transformations. 16
3.2 Translation vectors and equipoint transformations that define space group $F23$ . . . 17
3.3 Pseudo-code demonstrating the unit cell generation algorithm 18
3.4 A non-special point in in $Fm\bar{3}m$ generates 96 symmetry-required points 18

4.1 Scattering vectors. 20
4.2 Ewald sphere construction 23
4.3 Offset atom planes cause extinguishing of diffraction conditions 24
4.4 Atomic scattering factors 25
4.5 The Bragg diffraction condition. 26
4.6 Lorentz-polarization factor as a function of 2θ. 28

5.1 Pseudo-code describing the process of finding valid scattering vectors. 30
5.2 Pseudo-code showing the structure factor calculation algorithm. 30
5.3 Algorithm for converting structure factor values into a x-ray powder pattern 31
5.4 Calculated vs. experimental x-ray diffraction pattern of gold 32

6.1 Space group panel for the NaCl crystal structure. 34
6.2 The three atom list panels for the NaCl crystal structure. 35
6.3 NaCl crystal visualization in AtomicControl. 36
6.4 X-ray diffraction and reciprocal lattice of NaCl 37
6.5 The File menu of AtomicControl. 37

7.1 Space group panel of conventional BCC iron and resulting unit cell 40

7.2 Space group panel of primitive BCC Fe and resulting crystal structure 41

7.3 Diffraction patterns of conventional and primitive BCC unit cells 42

7.4 Space group panel with Cu_3Au lattice parameters entered. 43

7.5 Ordered Cu_3Au visualization 43

7.6 FCC copper unit cell visualization. 44

7.7 Comparison of x-ray powder diffraction of ordered and disordered Cu_3Au 45

7.8 Space group panel definition of austenite. 46

7.9 Space group panel definition of martensite. 47

7.10 The body-centered tetragonal lattice 47

7.11 Space group panel definition of BCT martensite. 47

7.12 Austenite and martensite x-ray diffraction patterns 48

Chapter 1

Introduction

1.1 Motivation

Learning crystallography and x-ray diffraction requires understanding 3D geometry, symmetry operations, and the abstract concept of a reciprocal space. These concepts require the student to visualize crystal structures in order to observe crystal symmetries and geometric constraints. Currently there is a need, especially in the MIT materials science undergraduate curriculum, for a freely available, intuitive tool to interactively build and visualize crystal structures as well as simulate x-ray diffraction patterns. Such a tool would be very useful to the student trying to visualize a crystal structure. Current tools are often very expensive or difficult to use, and often both. An easy to use alternative would make the subject of crystallography more accessible and easier to learn.

A commercial modeling package called Cerius^2 was used in the undergraduate Materials Structures Laboratory class (3.081) until 2003 as a way to build and visualize crystal structures and to do simple x-ray powder diffraction simulations. While Cerius^2 was previously available to the MIT community on the Silicon Graphics (SGI) Athena workstations,these SGI workstations have been phased out and students no longer have access to this package [1]. Since Cerius^2 is no longer available to MIT students, the students in 3.012 and 3.014 (the sophomore-level materials theory and laboratory classes) need a new tool to replace Cerius^2 , in order to do 3D crystal visualization and x-ray diffraction simulations.

Given the need for a crystal visualization and simulation package for use in the undergraduate materials science curriculum, this project's objective has been to produce an open-source software package that can both allow the user to build and visualize a crystal as well as produce a simulated x-ray diffraction pattern. This has been realized through a software program called AtomicControl. To provide cross-platform compatibility AtomicControl has been written in Java, and as a result can be run on any platform that supports Java, including Microsoft Windows, Apple's MacOS X, and GNU/Linux [2].

AtomicControl provides an interactive crystal builder that allows the user to design a crystal by defining its Bravais lattice, space group symmetry, and atom coordinates. It produces a 3D visualization of the constructed crystal structure. AtomicControl also provides an x-ray diffraction simulator. AtomicControl takes any arbitrary user-built crystal structure and calculates its x-ray power diffraction for the user. This allows for the student to interactively modify the crystal structure and observe the effect on the powder pattern.

1.2 Overview

This document discusses AtomicControl's two main features, the crystal builder and the diffraction simulator. Chapter 2 provides a brief description of the object-oriented software model used in the development of AtomicControl. Chapter 3 discusses the theory behind generating a crystal structure from a space group definition and describes the algorithm used in AtomicControl to generate the a crystal. An overview of basic x-ray diffraction theory is provided in Chapter 4 with a focus on the vector-based description. The algorithms used to produce x-ray powder diffraction patterns in AtomicControl are discussed in Chapter 5. Since this a program that is designed to be easy to use, a description of the user interface of AtomicControl is provided in Chapter 6. Lastly, lesson plans that demonstrate how AtomicControl may be used in a classroom are provided in Chapter 7.

Chapter 2

Software Model

AtomicControl is written in the Java programming language and is fully object-oriented. Since the Java platform is available on most operating systems AtomicControl may be used almost anywhere. AtomicControl can be run on any platform that supports Java, and has been tested on Microsoft Windows, Apple's MacOS X, and GNU/Linux.

The object-oriented nature of Java was leveraged in AtomicControl — each crystal, atom, element, space group is represented internally as a Java object. Each object encapsulates data and functionality inherent in its type. For example, AtomicControl can interrogate an `Atom` object to retrieve its position, its radius, or its charge. The central object representation is the `Crystal` class. A `Crystal` object contains lists of `Atom` objects that describe the crystal's generator atoms, its unit cell atoms, and all atoms in the crystal. The crystal also references one of the 230 `SpaceGroup` objects, each of which describes the transformations and translation vectors to build the required symmetry into the unit cell of that specific space group. Figure 2.1 details these and other connections between objects in AtomicControl.

This Java object structure is a useful way to keep track of data while AtomicControl is running, but in order to save and retrieve crystal information a file format is required. An extensible markup language (XML) file structure was used so that the files would be easy to create and parse in Java. XML is a hierarchical file format that has a standard method of parsing [3]. The saved data files for AtomicControl use the crystal as the top level in this hierarchy. For each crystal the lattice definition and atom lists are provided. Figure 2.2 shows the basic hierarchy of this file format.

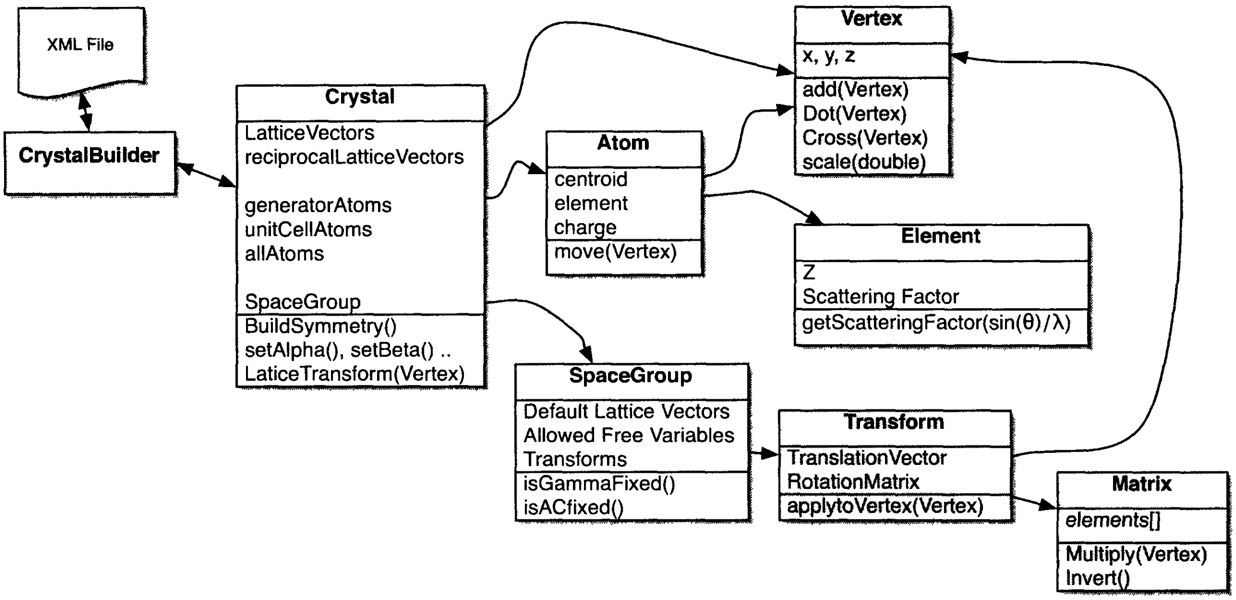
XML File
CrystalBuilder
Crystal
LatticeVectors
reciprocalLatticeVectors
generatorAtoms
unitCellAtoms
allAtoms
SpaceGroup
BuildSymmetry()
setAlpha(), setBeta() ..
LaticeTransform(Vertex)
Atom
centroid
element
charge
move(Vertex)
Vertex
x, y, z
add(Vertex)
Dot(Vertex)
Cross(Vertex)
scale(double)
Element
Z
Scattering Factor
getScatteringFactor(sin(θ)/λ)
SpaceGroup
Default Lattice Vectors
Allowed Free Variables
Transforms
isGammaFixed()
isACfixed()
Transform
TranslationVector
RotationMatrix
applytoVertex(Vertex)
Matrix
elements[]
Multiply(Vertex)
Invert()

Figure 2.1: Interaction of Java objects in AtomicControl

```
<crystal>
    <spacegroup id="1" />

    <latticevects>
        <a>
            <x>1</x> <y>0</y> <z>0</z>
        </a>
        <b>...</b>
        <c>...</c>
    </latticevects>

    <generatoratoms>
        <atom element="1" charge="0" visible="true">
            <centroid>
                <u>0</u> <v>0</v> <w>0</w>
            </centroid>
        </atom>
    ...
    </generatoratoms>

    <unitcellatoms> ... </unitcell>
    <allatoms> ... </all>
</crystal>
```

Figure 2.2: XML crystal file format.

Chapter 3

Space Group Symmetry Builder

3.1 Space group definition

Each space group is defined by unique set of symmetry operations, which result in a 3D periodic structure. 230 space groups have been proven via group theory to be exhaustive, i.e. they describe all possible symmetry combinations for periodically tiling space [4]. Because of this completeness, any crystal can be categorized into one of these 230. Space groups have a standardized naming and numbering convention that has been put forth in the International Tables of Crystallography [5]. The names describe the prominent symmetries present and the numbering scheme is logical: the higher numbered space groups correspond to higher symmetry systems. For example the lowest symmetry space group $P1$ (no. 1) has only translational symmetry. $P\bar{1}$ (no. 2) has an additional inversion symmetry point about the origin. Higher symmetry space groups will include mirror and rotational symmetries along with more complex symmetries such as glide planes. All of these types of symmetry operations can be described by geometrical constructions as well as mathematical transformations, known as equipoint transformations. These transformations are very useful because they are easy for a computer program to implement. Thus AtomicControl uses these equipoint transformations to generate a crystal unit cell [6]. These equipoint transformations are of the form $\vec{x'} = [R]\vec{x} + \vec{T}$:

$$\begin{bmatrix} u' \\ v' \\ w' \end{bmatrix} = \begin{bmatrix} R_{11} & R_{12} & R_{13} \\ R_{21} & R_{22} & R_{23} \\ R_{31} & R_{32} & R_{33} \end{bmatrix} \begin{bmatrix} u \\ v \\ w \end{bmatrix} + \begin{bmatrix} T_1 \\ T_2 \\ T_3 \end{bmatrix} \tag{3.1}$$

where $\vec{x}$ is the atom location in fractional coordinates, and $\vec{x'}$ is an atom position that must exist to satisfy the symmetry operation. T is restricted to vectors within the unit cell (smaller than [1 1 1]). This restriction on T ensures that the number of transformations required to fully describe the unit cell is finite.

There is an additional requirement to fully define the unit cell when the unit cell is not primitive. In these cases translation operators are required to create the multiple lattice points in a non-primitive unit cell definition. For example, the conventional FCC lattice has four lattice points per cell. This means that defining this unit cell requires three additional translation vectors $(\frac{1}{2}, \frac{1}{2}, 0), (\frac{1}{2}, 0, \frac{1}{2}), (0, \frac{1}{2}, \frac{1}{2})$.

3.2 Symmetry operators and their matrix representations

Equipoint transformations can in some cases be directly correlated with a standard crystallographic symmetry operator. For example, an inversion symmetry through the origin can be represented as the negative identity matrix, while a *uv*-plane mirror can be described by a matrix that flips the w component of $\vec{x}$. Glide symmetries, while more complex, can still be represented through two operators: a matrix operation and a subsequent translation. Figure 3.1 provides some examples of a symmetry operator and its equipoint transformation.

Inversion	*uv*-plane mirror	Glide
$R = \begin{bmatrix} -1 & 0 & 0 \\ 0 & -1 & 0 \\ 0 & 0 & -1 \end{bmatrix}$	$R = \begin{bmatrix} 1 & 0 & 0 \\ 0 & 1 & 0 \\ 0 & 0 & -1 \end{bmatrix}$	$R = \begin{bmatrix} 1 & 0 & 0 \\ 0 & 1 & 0 \\ 0 & 0 & -1 \end{bmatrix}; \vec{T} = \begin{bmatrix} \frac{1}{2} \\ 0 \\ 0 \end{bmatrix}$

Figure 3.1: Various symmetry operators represented as vector transformations.

A space group can be defined as a finite set of such transformations. This does not mean that every symmetry in the crystal needs to be represented as a separate transformation. For example a four-fold axis can also be part of two intersecting orthogonal mirror planes, and symmetry transformations for the four-fold axis will be redundant. There is a minimum number of transformations required to fully define the space group and an example is shown in Fig. 3.2.

```
 Translation vectors : (0,0,0), (1/2,1/2,0), (0,1/2,1/2), (1/2,0,1/2)
+------------------------------------------------------------------------------+
| 12 equipoint transformations (X)'=[R]*(X)+(T) :                              |
+------------------------------------------------------------------------------+
| R(11) R(12) R(13) R(21) R(22) R(23) R(31) R(32) R(33)    T(1)   T(2)   T(3)  |
| 1.0   0.0   0.0   0.0   1.0   0.0   0.0   0.0   1.0    0.000  0.000  0.000  |
| 1.0   0.0   0.0   0.0  -1.0   0.0   0.0   0.0  -1.0    0.000  0.000  0.000  |
|-1.0   0.0   0.0   0.0   1.0   0.0   0.0   0.0  -1.0    0.000  0.000  0.000  |
|-1.0   0.0   0.0   0.0  -1.0   0.0   0.0   0.0   1.0    0.000  0.000  0.000  |
| 0.0   1.0   0.0   0.0   0.0   1.0   1.0   0.0   0.0    0.000  0.000  0.000  |
| 0.0  -1.0   0.0   0.0   0.0  -1.0   1.0   0.0   0.0    0.000  0.000  0.000  |
| 0.0   1.0   0.0   0.0   0.0  -1.0  -1.0   0.0   0.0    0.000  0.000  0.000  |
| 0.0  -1.0   0.0   0.0   0.0   1.0  -1.0   0.0   0.0    0.000  0.000  0.000  |
| 0.0   0.0   1.0   1.0   0.0   0.0   0.0   1.0   0.0    0.000  0.000  0.000  |
| 0.0   0.0  -1.0   1.0   0.0   0.0   0.0  -1.0   0.0    0.000  0.000  0.000  |
| 0.0   0.0  -1.0  -1.0   0.0   0.0   0.0   1.0   0.0    0.000  0.000  0.000  |
| 0.0   0.0   1.0  -1.0   0.0   0.0   0.0  -1.0   0.0    0.000  0.000  0.000  |
+------------------------------------------------------------------------------+
```

Figure 3.2: Translation vectors and equipoint transformations that define space group no. 196, $F23$, the lowest symmetry face-centered cubic space group [7].

3.3 Algorithm for crystal generation

A space group's equipoint transformations can be applied to any atom in a crystal to produce new atom positions required by symmetry. In AtomicControl this property is used to build the unit cell of the crystal. All the user-defined generator atoms have the list of transformations applied to their fractional coordinates. This process produces a larger list of atoms, some of which are duplicates, i.e. they occur at the same spatial location. These duplicates are then removed by searching through the atom list. This process of transformation application and duplicate removal is repeated until the atom list stabilizes. Once stabilized the list of atoms contains the full unit cell as well as some valid atoms in the neighboring cells. The list is truncated to contain only unit cell atoms, and unit cell is then complete. This crystal building process process is outlined in Fig. 3.3.

```
Apply translation vectors to generator atom list
do:
    for each atom:
       for each transformation:
           apply transformation to atom
           create a copy of the atom at the transformed coordinate
    remove duplicates from atom list
while atom list is bigger than before, repeat do
remove atoms outside the unit cell
```

Figure 3.3: Pseudo-code demonstrating the unit cell generation algorithm

3.4 Crystal generation results

For a non-special atom position in an $Fm\bar{3}m$ symmetry crystal there will be 96 atom positions that must be filled in order to conform to the symmetry of $Fm\bar{3}m$. To make sure that AtomicControl can generate these 96 symmetry-required points, an arbitrary non-special generator atom had $Fm\bar{3}m$ symmetry imposed on it. It can be seen in Fig. 3.4 that AtomicControl has correctly generated all 96 symmetry-required points to fully define the unit cell.

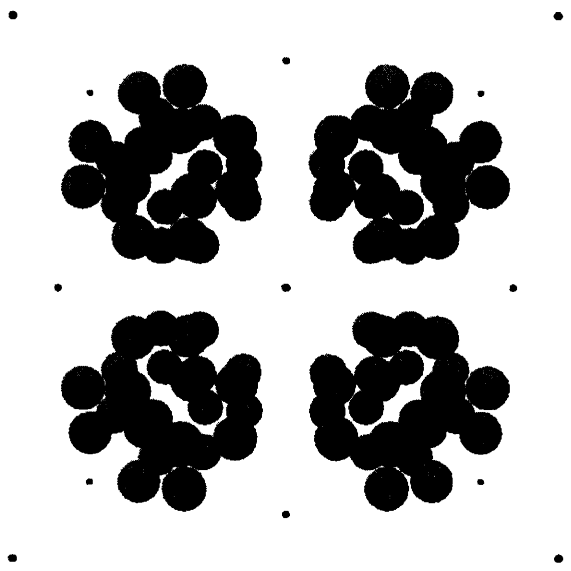

Figure 3.4: A non-special point in $Fm\bar{3}m$ generates 96 symmetry-required points. Small dots are the lattice points.

Chapter 4

X-ray Diffraction Theory

X-ray diffraction is based on the assumption that x-ray radiation with wavelengths on the order of Ångstroms can elastically scatter off the electronic structure of a crystal. The periodicity of the crystal will cause this scattering of the x-ray plane-wave to constructively interfere at certain scattering directions while destructively interfering at other scattering directions. The diffracted x-rays are detected at a distance much larger than the periodicity of the lattice, so that the diffraction can be approximated by the Fraunhofer diffraction conditions [8]. By using this model it has been shown that the diffraction conditions are related to the Fourier transform of the electronic structure [9]. The Fourier transform allows the calculation of the complex amplitude A as a function of the elastic scattering vector $\vec{\Delta k}$, as shown in Eq. 4.1.

$$A(\vec{\Delta k}) = \int \rho(\vec{x}) e^{-i\vec{\Delta k}\cdot\vec{x}} dv_{\vec{x}} \tag{4.1}$$

Where:

$$\vec{\Delta k} = \vec{k'} - \vec{k} \tag{4.2}$$

$$|\vec{k}| = |\vec{k'}| = \frac{2\pi}{\lambda} \tag{4.3}$$

The scattering vector's meaning can be best described graphically, as in Fig. 4.1 where $\vec{k}$ is the incoming wave-vector, $\vec{k'}$ is the scattered wave-vector and $\vec{\Delta k}$ is their difference. For elastic scattering $\vec{k}$ and $\vec{k'}$ must have the same length to conserve the wavelength and therefore the energy of the photon. The vector difference between these is known as the scattering vector $\vec{\Delta k}$, which represents the momentum the crystal must impart on the photon to cause the particular scattering condition.

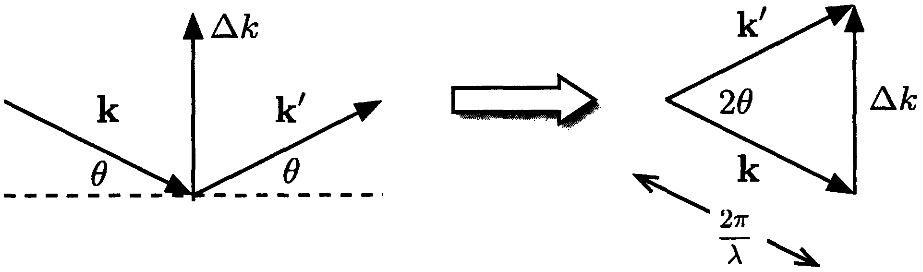

Figure 4.1: Scattering vectors.

Integrating over all space for an infinite electron distribution, $\rho(\vec{x})$, is impossible, but some approximations can simplify the process. By assuming that the crystal is perfect and that each unit cell has the same electronic structure Eq. 4.1 can be reduced to a finite integral. If this assumption is made the electronic structure, $\rho(\vec{x})$, can be rewritten as a sum $\sum_n \rho_{\text{unitcell}}(\vec{x} - \vec{R_n})$, where R_n is a lattice vector of the form $R_n = m_1\vec{a}_1 + m_2\vec{a}_2 + m_3\vec{a}_3$, m_i are integers, and ρ_{unitcell} is the electronic structure of the unit cell. Equation 4.1 can then be rewritten as

$$A(\vec{\Delta k}) = \int \sum_n \rho_{\text{unitcell}}(\vec{x} - \vec{R_n}) e^{-i\vec{\Delta k}\cdot\vec{x}} dv_{\vec{x}} \tag{4.4}$$

By reordering the sum and the integral in Eq. 4.4, it can be rewritten as

$$A(\vec{\Delta k}) = \sum_n e^{-i\vec{\Delta k}\cdot\vec{x_n}} \int \rho_{\text{unitcell}}(\vec{x} - \vec{R_n}) e^{-i\vec{\Delta k}\cdot(\vec{x}-\vec{R_n})} dv_{\vec{x}} \tag{4.5}$$

Since $\int dv_{\vec{x}}$ is over all space, the shift by $\vec{R_n}$ does not affect the outcome, and Eq. 4.5 becomes

$$A(\vec{\Delta k}) = \sum_n e^{-i\vec{\Delta k}\cdot\vec{R_n}} \int \rho_{\text{unitcell}}(\vec{x}) e^{-i\vec{\Delta k}\cdot\vec{x}} dv_{\vec{x}} \tag{4.6}$$

This equation has simplified the Fourier transform to a finite sized integral, but it has a sum of phase factors in front that must be dealt with. Understanding the dot product $\vec{\Delta k} \cdot \vec{x}$ is important to understanding this sum. The definition of the reciprocal lattice can help in interpreting this quantitity.

4.1 The reciprocal lattice

The Fourier transform of a set of periodic delta functions is another set of periodic delta functions. Because of this property, it is convenient to define a reciprocal lattice that exists in Fourier space. A crystal lattice may be transformed into a lattice in Fourier (or reciprocal) space. This reciprocal lattice can be defined using basis vectors $(\vec{b_1}, \vec{b_2}, \vec{b_3})$, just like the real-space basis vectors,$(\vec{a_1}, \vec{a_2}, \vec{a_3})$, and the relationship between them is given by

$$\vec{a_i} \cdot \vec{b_j} = 2\pi\delta_{ij} \tag{4.7}$$

This creates the reciprocal lattice vectors $\vec{G}$ which are integer sums of the basis set $\vec{b_i}$ defined as

$$\vec{G} = h\vec{b_1} + k\vec{b_2} + l\vec{b_3} \tag{4.8}$$

where

$$\vec{b_1} = 2\pi\frac{\vec{a}_2 \times \vec{a}_3}{\vec{a}_1 \cdot \vec{a}_2 \times \vec{a}_3} \qquad \vec{b_2} = 2\pi\frac{\vec{a}_3 \times \vec{a}_1}{\vec{a}_1 \cdot \vec{a}_2 \times \vec{a}_3} \qquad \vec{b_3} = 2\pi\frac{\vec{a}_1 \times \vec{a}_2}{\vec{a}_1 \cdot \vec{a}_2 \times \vec{a}_3} \tag{4.9}$$

The definition of the reciprocal lattice leads to some useful properties. The dot product of any $\vec{G}$ and an arbitrary vector $\vec{x} = u\vec{a_1} + v\vec{a_2} + w\vec{a_3}$ is

$$\vec{G} \cdot \vec{x} = 2\pi(hu + kv + lw) \tag{4.10}$$

In the special case when $\vec{x}$ equals a lattice vector $\vec{R}$ defined as

$$\vec{R} = m_1\vec{a}_1 + m_2\vec{a}_2 + m_3\vec{a}_3 \text{ where } m_i \text{ are integers} \tag{4.11}$$

the dot product from Eq. 4.10 becomes

$$\vec{G} \cdot \vec{R} = 2\pi(m_1u + m_2v + m_3w) = N2\pi \text{ where } N \text{ is an integer} \tag{4.12}$$

This result has strong implications when this dot product is seen in a complex exponential.

The first term of Eq. 4.6, $\sum_n \exp(-i\Delta\vec{k} \cdot \vec{R_n})$, is closely related to the reciprocal lattice. Assuming an infinite crystal, this sum can only be non-zero if the phase factors do not cancel over the infinite sum over all lattice points R_n. It turns out that only when $\Delta\vec{k} \cdot \vec{R_n} = 2\pi$ for any lattice vector $\vec{R_n}$ does this sum become non-zero. This requirement looks strikingly similar to the definition of the reciprocal lattice in Eq. 4.12. This shows that the only allowed scattering vectors are reciprocal lattice vectors and that the diffraction amplitude $A(\vec{\Delta k})$ is non-zero only for $A(\vec{G})$. $A(\vec{\Delta k})$ can now be described as

$$A(\vec{\Delta k}) = \begin{cases} \int \rho_{\mathrm{unitcell}}(\vec{x}) e^{-i\vec{\Delta k}\cdot\vec{x}} dv_{\vec{x}} & \text{if} \vec{\Delta k} = \vec{G} \\ \\ 0 & \text{otherwise} \end{cases} \tag{4.13}$$

4.2 Ewald sphere construction

Given the requirement that $|\vec{k}| = |\vec{k'}| = 2\pi/\lambda$, but allowing all possible scattering angles, the locus of all potential scattering vectors can be plotted in reciprocal space. This locus is a sphere superimposed on the reciprocal lattice and is known as the Ewald sphere. This spherical shell is the region in Fourier space probed by the x-ray beam at a given wavelength and orientation with respect to the crystal. As discussed previously, only $\vec{\Delta k} = \vec{G}$ are allowed for diffraction. This further limits the possible scattering vectors. As is seen in Fig. 4.2a, the Ewald sphere is unlikely to intersect two reciprocal lattice points and form a diffraction condition, therefore there is a need to move the sphere to probe more of reciprocal space as seen if Fig. 4.2b.

Laue diffraction probes this space by using a spectrum of wavelengths. This has the effect of changing the radius of the shell, thus probing a solid sphere in reciprocal space. A powder diffraction experiment uses monochromatic x-rays, but each powder grain is oriented differently to incident beam. As the orientation of the crystal changes with respect to the incident beam, the Ewald sphere rolls in reciprocal space, as can be seen in the change between Fig. 4.2a and 4.2b. If all possible orientations are considered the Ewald sphere will sweep a limiting sphere with a radius of $4\pi/\lambda$. All reciprocal lattice vectors within this sphere can create diffraction peaks in a powder pattern.

4.3 Structure factor

So far the Fourier transform $A(\vec{\Delta k})$ of electronic structure has been simplified to a finite integral, but another assumption can be made to completely eliminate the need for the integral. It is possible to assume that an atom's electron distribution is localized around its nucleus. With this assumption the electron distribution of each atom with index i can be expressed as a scaled delta

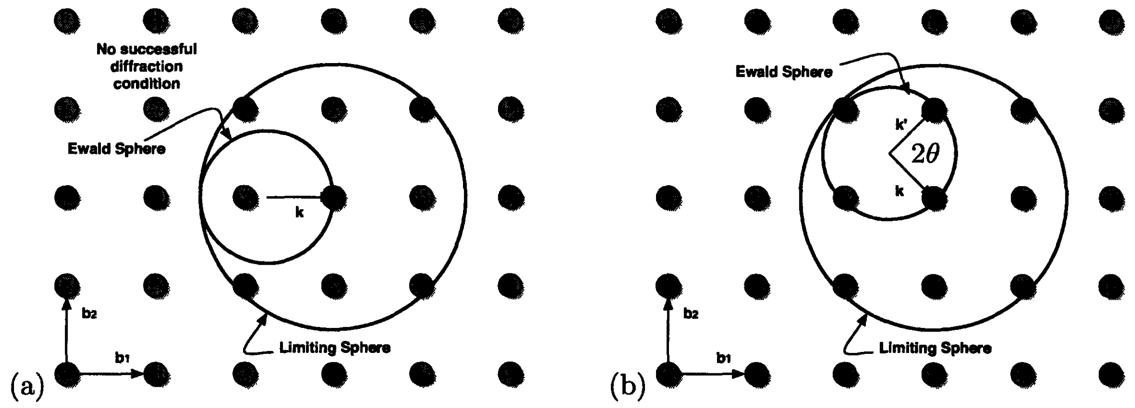

Figure 4.2: Ewald sphere construction showing a successful diffraction condition and an incident wave $\vec{k}$ that fails to create a diffraction condition. Most incident $\vec{k}$ will not produce a diffraction condition.

function $f_i\delta(\vec{x}-\vec{x_i})$, where $\vec{x_i}$ is the location of atom i and f_i is the scattering power of that atom. In this approximation $\rho_{\text{unitcell}}(\vec{x})$ can be expressed as $\sum_i f_i\delta(\vec{x}-\vec{x_i})$. Applying this approximation to Eq. 4.13 produces

$$A(\vec{G}) = \int \sum_i f_i(\vec{G})\delta(\vec{x}-\vec{x_i})e^{-i\vec{G}\cdot\vec{x}}dv_{\vec{x}} = \sum_i f_i e^{-i\vec{G}\cdot\vec{x_i}} \tag{4.14}$$

This definition of $A(\vec{G})$ is known as the structure factor because it defines the diffraction amplitude in terms of the atomic structure of the unit cell. The structure factor describes the diffraction amplitude $A(\vec{G})$ as a sum of phase-factors due to phase-offsets from the scattering of x-rays off of atoms in the unit cell.

Any scattering vector represented by a reciprocal lattice vector in the limiting sphere represents a *possible* diffraction condition. Each of these reciprocal lattice vectors represents a periodicity in the real-space crystal lattice. This periodicity is created due to repeated planes of atoms. If there is an extra atom plane between the atom planes defined by the *hkl* of the reciprocal lattice vector, the scattering off of the extra plane can destructively interfere with the scattered photons from the planes and extinguish the diffraction amplitude as seen in Fig. 4.3.

4.4 Atomic scattering factor

Each element or ion has a scattering power associated with it due to its electronic structure, and its power to either constructively or destructively interfere in a diffraction pattern is scaled by this power. This means that a carbon atom will have approximately half the scattering ability of a

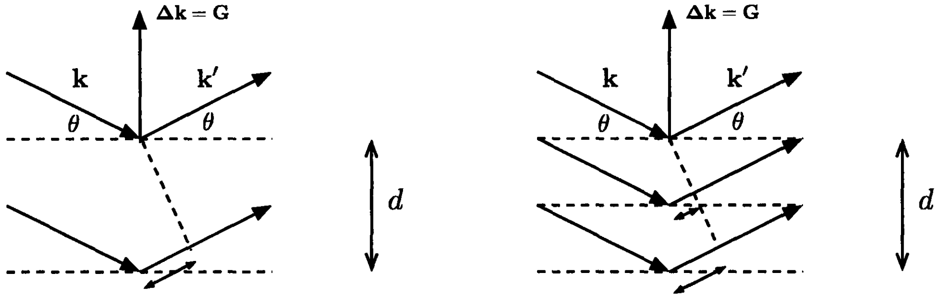

Constructively Interfere

Destructively Interfere

Figure 4.3: The addition of an offset plane of atoms causes destructive interference of scattered photons.

sulfur atom simply because it has half the number of electrons. This difference is quantified in the atomic scattering factor, f, which is the defined as the scattering power compared to a single electron [10]:

$$f = \frac{\text{scattering power of atom}}{\text{scattering power of a single electron}} \tag{4.15}$$

All of the discussion about structure factors has used the assumption that atoms are infinitesimal points, but in reality there is an electron distribution that is usually spherically symmetric about the nucleus. It is possible to take this into account by calculating the diffraction pattern as the Fourier transform of this continuous electronic structure, as desribed in 4.1. However this complexity is not needed for most calculations — and not possible if the electronic structure is not known — so this detail can be parameterized into the atomic scattering factor. When the diffraction angle increases, the x-rays interact with the outer parts of the electron cloud and therefore have less scattering power. Therefore the atomic scattering factor, f, can be parameterized as a function of diffraction angle. The atomic scattering factors for elements and ions are tabulated as a function of $\sin\theta/\lambda$ which is related to the magnitude of the scattering vector $\vec{\Delta k}$. There is no directional dependence tabulated because these values assume that the electronic structures are spherically symmetric. AtomicControl uses these tabulated values and interpolates to find the appropriate scattering power for the situation. Figure 4.4 shows the atomic scattering factors for a number of elements as they are used in AtomicControl. AtomicControl uses a linear interpolation method to find the scattering factor for an arbitrary scattering angle.

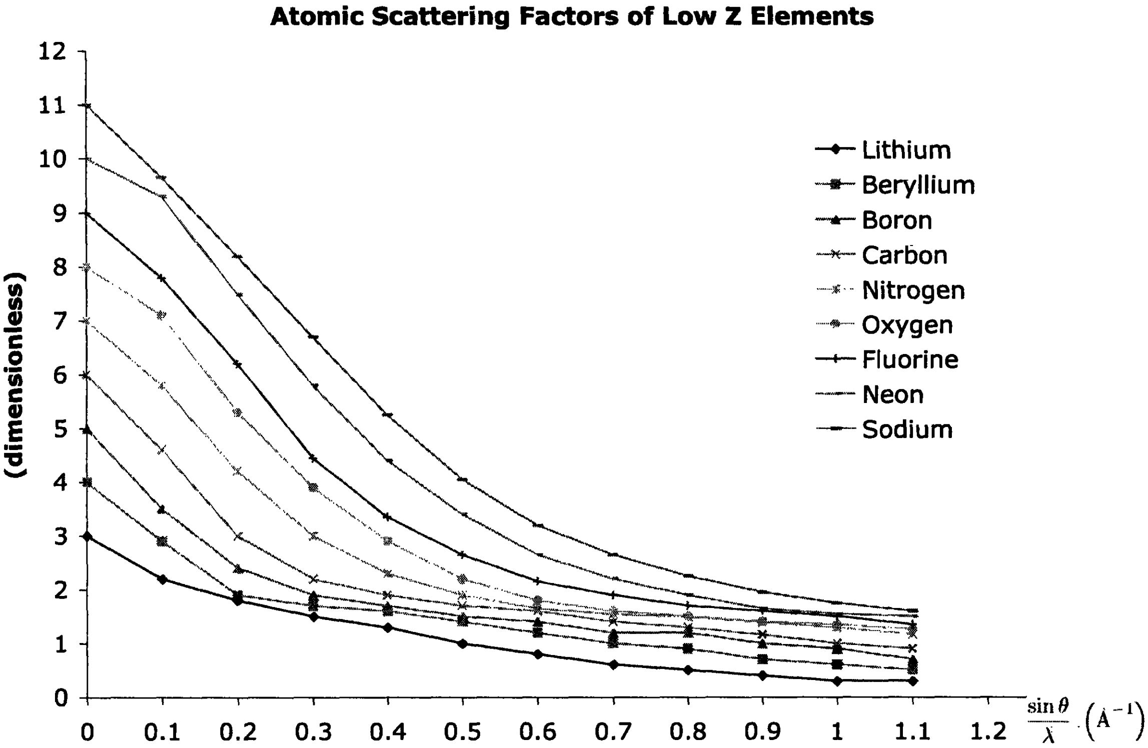

Figure 4.4: The atomic scattering factor of a number of elements as a function of $\sin\theta/\lambda$ [10].

4.5 Ideal powder pattern

A powder pattern is an a spectroscopic image of a crystalline powder bombarded with monochromatic x-rays. As seen in the Ewald sphere description of diffraction, the likelihood of a diffraction condition occurring is very slight for a single crystal with a single beam of monochromatic x-rays probing the sample. The powder diffraction method addresses this problem by creating many orientations of the crystal in the path of the x-rays. An ideal powder pattern has all possible orientations equally available, and this has the effect of probing every point in the limiting sphere by rolling the Ewald sphere in reciprocal space. However, there is a drawback to this method of probing reciprocal space. The powder pattern superimposes all diffraction conditions which have the same scattering angle θ.

A more conventional perspective on the powder pattern is provided with Bragg's formula. The Bragg condition occurs when $\phi = 2\pi$, that is when the scattered photons are in phase, and the condition $\lambda = 2d \sin\theta$ is obeyed. In a powder pattern, each observed diffraction peak in 2θ is associated with a given lattice spacing via Bragg's formula: $d = \lambda/(2\sin\theta)$. As previously discussed, each reciprocal lattice vector is associated with a lattice spacing in the crystal and it also represents

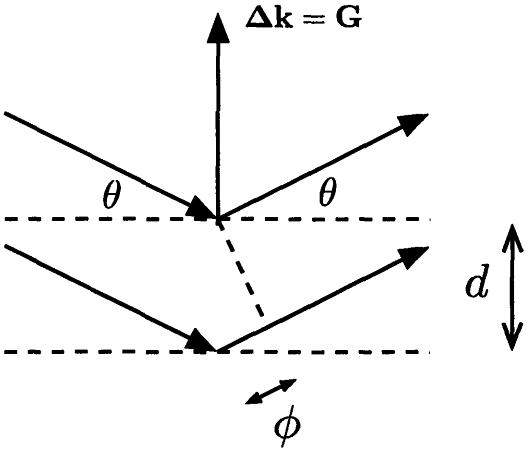

Figure 4.5: The Bragg diffraction condition. $\phi = 2\pi$ when $\lambda = 2d\sin\theta$.

the elastic change in wave-vector of a diffracted photon, $(\vec{\Delta k})$ as shown in the construction in Fig. 4.5. Lattice spacing, diffraction angle, and associated reciprocal lattice vector can be all associated. While the Bragg definition of diffraction angle is useful in understanding, the association between reciprocal lattice vector and angle will be useful in computing the powder diffraction pattern in AtomicControl via the relation

$$2d = \frac{\sin\theta}{\lambda} = \frac{|\vec{\Delta k}|}{4\pi} = \frac{|\vec{G}|}{4\pi} \tag{4.16}$$

The magnitude of diffraction peaks at a given 2θ angle is determined by the sum of all $A(\vec{G})$ which have the same scattering angle, 2θ. The intensity observed is related to A^2 and can be represented by a number of factors that are based on the geometry of the crystal, the geometry of the diffraction apparatus, and the electronic structure of the crystal. For the standard diffractometer setup the following components must be considered: structure factor, as previous discussed; the multiplicity; and the Lorentz-polarization factor in the form

$$\underbrace{I}_{\text{Relative Intensity}} = \underbrace{|F|^2}_{\text{Structure Factor}} \cdot \underbrace{p}_{\text{Multiplicity}} \cdot \underbrace{\left(\frac{1+\cos^2 2\theta}{\sin^2\theta\cos\theta}\right)}_{\text{LP factor}} \tag{4.17}$$

Multiplicity

Due to the symmetry of the crystal, there is always more than one reciprocal lattice vector, $\vec{G}$, that is associated with the same scattering angle. For example, the (111) plane will always have the same scattering angle as $(\bar{1}\bar{1}\bar{1})$. However, the multiplicity however can also be larger than two. In a cubic system the (100) plane is in a family of six diffraction-equivalent planes. In an tetragonal system (100) and (010) fall under the same family and have the same diffraction angle, but the (001) and $(00\bar{1})$ are in a separate family and have a different diffraction angle due to a different inter-planar spacing d. In an orthorhombic crystal, the multiplicity drops to two for each of the $\{100\}$,$\{010\}$, and $\{001\}$, because each has different d. AtomicControl does not require an explicit calculation of multiplicities when calculating diffraction intensities because it considers all allowed scattering vectors in *all* directions and simply adds the structure factors when it finds ones that have the same 2θ angle.

Lorentz-polarization factor

The Lorentz-polarization factor is a combination of a number of geometric terms that arise from experimental broadening of diffraction peaks, as well as the polarization of diffracted photons. These combine to decrease the intensity of photons diffracted at mid-range angles and has the form

$$\text{L.P.} = \left(\frac{1+\cos^2 2\theta}{\sin^2\theta\cos\theta}\right) \tag{4.18}$$

A plot of the Lorentz-polarization factor as a function of scattering angle is shown in Fig. 4.6.

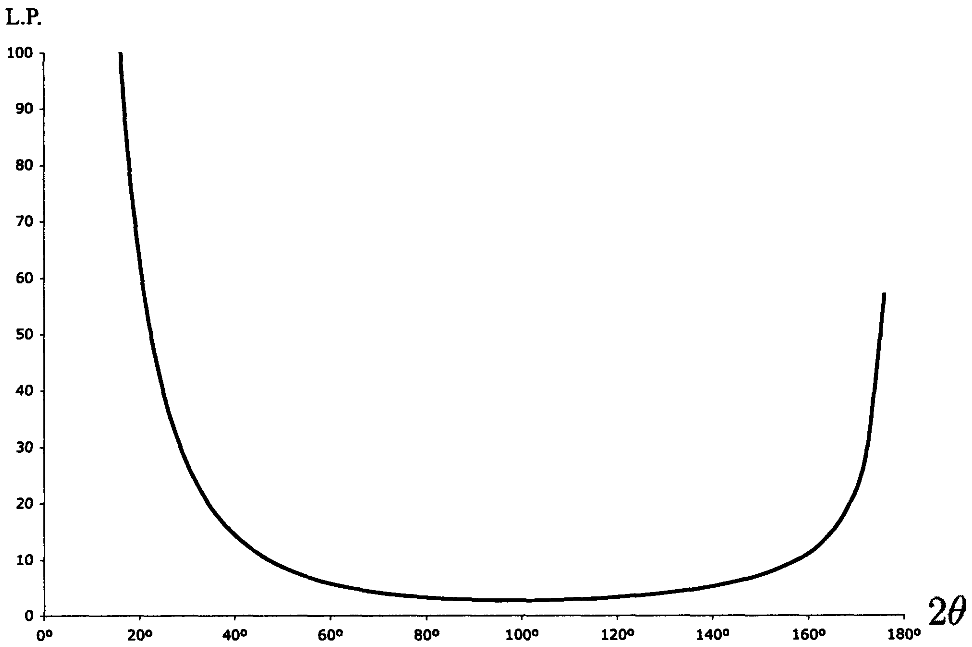

Figure 4.6: Lorentz-polarization factor as a function of 2θ.

Chapter 5

X-ray Powder Diffraction Pattern Algorithm

5.1 Finding valid scattering vectors

The first step to calculating an x-ray powder diffraction pattern is to find which scattering conditions are possible. As described earlier, only scattering vectors $\vec{\Delta k} = \vec{G}$ are allowed for diffraction off an infinite crystal. The are still an infinite number of $\vec{G}$'s, but with elastic scattering only a small subset is allowed with monochromatic radiation. This was shown geometrically in Fig. 4.1. This geometry relates angle to the reciprocal lattice vector by the relation

$$\frac{\sin\theta}{\lambda} = \frac{|G|}{4\pi} \tag{5.1}$$

If $|\vec{G}| > 4\pi/\lambda$ then $\vec{G}$ is outside the limiting sphere, and the associated interplanar spacing is not probed by the diffractometer. AtomicControl calculates, based on λ, a maximum value for h, k, and l that could yield a valid scattering vector. From the the range from $[-h_{\max}\ -k_{\max}\ -l_{\max}]$ to $[h_{\max}\ k_{\max}\ l_{\max}]$, a list of allowed $\vec{G}$ vectors within can be found by checking their magnitude as outlined in Fig. 5.1.

```
for each $h$ from $-h_{\max}$ to $h_{\max}$:
    for each $k$ from $-k_{\max}$ to $k_{\max}$:
        for each $l$ from $-l_{\max}$ to $l_{\max}$:
            Gmag = $|h\vec{b}_1 + k\vec{b}_2 + l\vec{b}_3|^2$
            if Gmag$\cdot\lambda/4\pi$ $<$ 1 :
                add [h k l] to list of allowed $\vec{G}$
```

Figure 5.1: Pseudo-code describing the process of finding valid scattering vectors.

5.2 Calculation of structure factors

Once the allowed scattering vectors (reciprocal lattice vectors, $\vec{G}$) are found, it is possible to calculate a structure factor a for each using the definition of the unit cell. In the process outlined in Fig. 5.2, AtomicControl iterates through all allowed $\vec{G}$'s and for each $\vec{G}$ it iterates through all unit cell atoms to produce the sum

$$F(\vec{G}) = \sum_{j}^{\text{unit cell}} f_j(\vec{G})\ e^{i\vec{G}\cdot\vec{R}_j} \tag{5.2}$$

```
for each allowed $\vec{G}_i$ :
    for each unit cell atom$_j$:
        $\vec{R}_j$ = Atom$_j$'s Centroid
        $s$ $=$ $|\vec{G}_i|/4\pi$
        $F_i$ = $F_i$ $+$ $f_j(s)$ $e^{\vec{R}_j\cdot\ \vec{G}_i}$
    save $F_i$
```

Figure 5.2: Pseudo-code showing the structure factor calculation algorithm.

5.3 Converting structure factors to powder pattern

The final step in producing a powder diffraction pattern is to sort the structure factors into their associated diffraction angles. The diffraction angle is calculated based on the relationship

$$\theta = \sin^{-1}\left(\frac{\lambda|\vec{G}|}{4\pi}\right) \tag{5.3}$$

Once this angle θ_i is found, the current G_i's structure factor is superimposed on the intensity at $2\theta_i$ until all allowed G_i's have been exhausted. Once the sorting process is complete the Lorentz-polarization factor is then applied to the plot values. This sorting process is outlined in Fig. 5.3.

If an disallowed G_i is run through this algorithm, the algorithm would try to take the arc sine

```
for each $\vec{G_i}$ :
        $\theta_i = \sin^{-1}( \frac{\lambda\ |\vec{G_i}|}{4\pi} )$
    $I(2\theta_i) = I(2\theta_i) + |F_i|^2$
for each $\theta_n$ :
    $I(2\theta_n) = I(2\theta_n) * LP(\theta_n)$
```

Figure 5.3: Pseudo-code showing the algorithm for converting structure factor values into a x-ray powder pattern plot.

of a value greater than one. Java handles this condition by giving the result as zero. However, the correct result would be a complex angle that would be meaningless in this context. It is also important to note that this algorithm does not contain any multiplication by a multiplicity because it does not need to. AtomicControl does not need to explicitly calculate multiplicities when calculating diffraction intensities because it considers all allowed scattering vectors and simply adds the structure factors when it finds ones that have the same 2θ angle.

5.4 Results of diffraction calculations

To verify AtomicControl's method of x-ray powder diffraction calculation, known structures were simulated and compared with experimental powder patterns. AtomicControl has been tested with a number of cubic structures including FCC gold, BCC iron, CdTe, and NaCl. Hexagonal elemental structures such as magnesium were also tested. The diffraction patterns for these compounds matched well with experiment. An illustrative example is shown in Fig. 5.4. As time permits a wider range of structures will be tested on AtomicControl to assure that the algorithm is error-free.

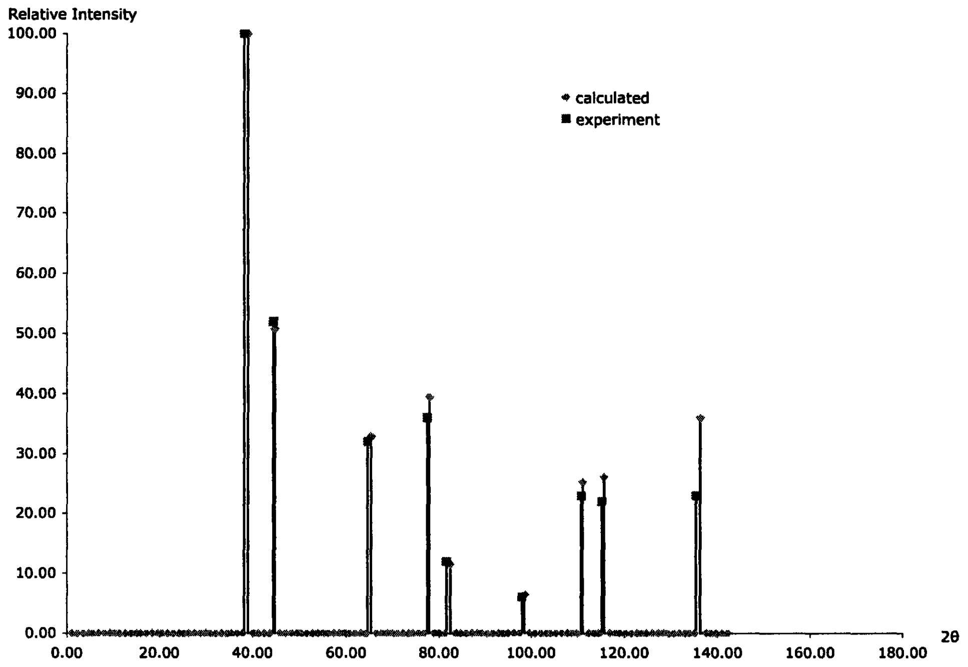

Figure 5.4: The powder pattern of gold: calculated in AtomicControl vs. experiment from Swanson and Tatge [11].

Chapter 6

User Interface

AtomicControl is designed to be a user-friendly program so that the learning curve of the software does not inhibit learning of crystallography. Because of this AtomicControl's interface is organized to the logical steps of building a crystal model, starting with the specification of a space group and lattice parameters, then the adding of unit cell, and finishing with the generation of x-ray power diffraction patterns. This process, however, is not rigid. The user can modify the crystal at any of these stages in the process at any time and AtomicControl will automatically update the crystal based on the change. This type of instant feedback is a very useful feature that can help especially when this application is used for teaching purposes.

6.1 Specifying a space group

The first step in this process of building a crystal is to specify the crystal's space group, lattice constants, and interaxial angles. The first panel that the user sees on opening AtomicControl is the space group panel. The space group panel lets the user choose a crystal system and a space group within that system. Each crystal system has a set of constraints that make it unique. For example a cubic system must have all interaxial angles at 90^o and the lattice constants equal. The space group panel knows this and will not allow the user to change the fixed interaxial angles and keeps the lattice constants synchronized by making sure lattice-constant ratios are maintained at the crystal system specification. A screenshot of the space group panel is provided in Fig. 6.1.

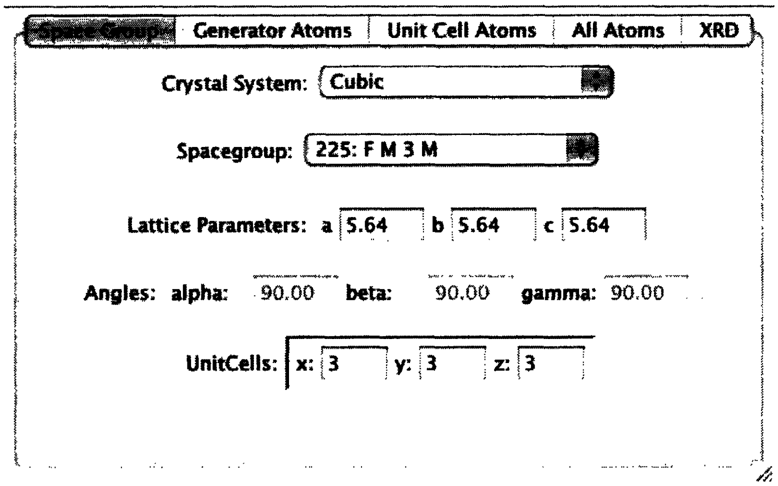

Crystal System: Cubic

Spacegroup: 225: F M 3 M

Lattice Parameters: a 5.64 b 5.64 c 5.64

Angles: alpha: 90.00 beta: 90.00 gamma: 90.00

UnitCells: x: 3 y: 3 z: 3

Figure 6.1: Space group panel for the NaCl crystal structure.

6.2 Populating the unit cell

Once the space group and lattice parameters are defined, the user can then add atoms to the unit cell. Clicking the "Add Generator Atom" button in the generator panel will create a default atom shown in the panel. The atoms fractional coordinates, element type, charge, and visibility in the crystal viewer, can be modified from this panel as seen in Fig. 6.2. The choice of element type and charge will affect the radius observed in the crystal viewer as well as affect the atomic scattering factor used in the calculation of the x-ray diffraction pattern.

The atoms in this panel will have the space group symmetry operators applied to produce the unit cell atoms, which are displayed in the unit cell atoms panel. Additionally, the unit cell atoms will be translated and copied to produce the multi-celled crystal in the all atoms panel. Each time the user changes a generator atom, the unit cell atoms are automatically recalculated and the user will see changes immediately in the crystal viewer.

6.3 Viewing the crystal

When the user is defining the space group and the generator atoms, the rest of the crystal data is automatically updated. This means that as soon as the user adds an atom, he can see the results instantly in the crystal viewer. The crystal viewer can show the entire crystal, a single unit cell, or just the generator atoms defined by the user. The view can be zoomed and the relative size of the atoms to the lattice constant can be changed to go from a space-filling model to a point structure. The main feature of the crystal viewer is the ability for the user to click and drag on the crystal and

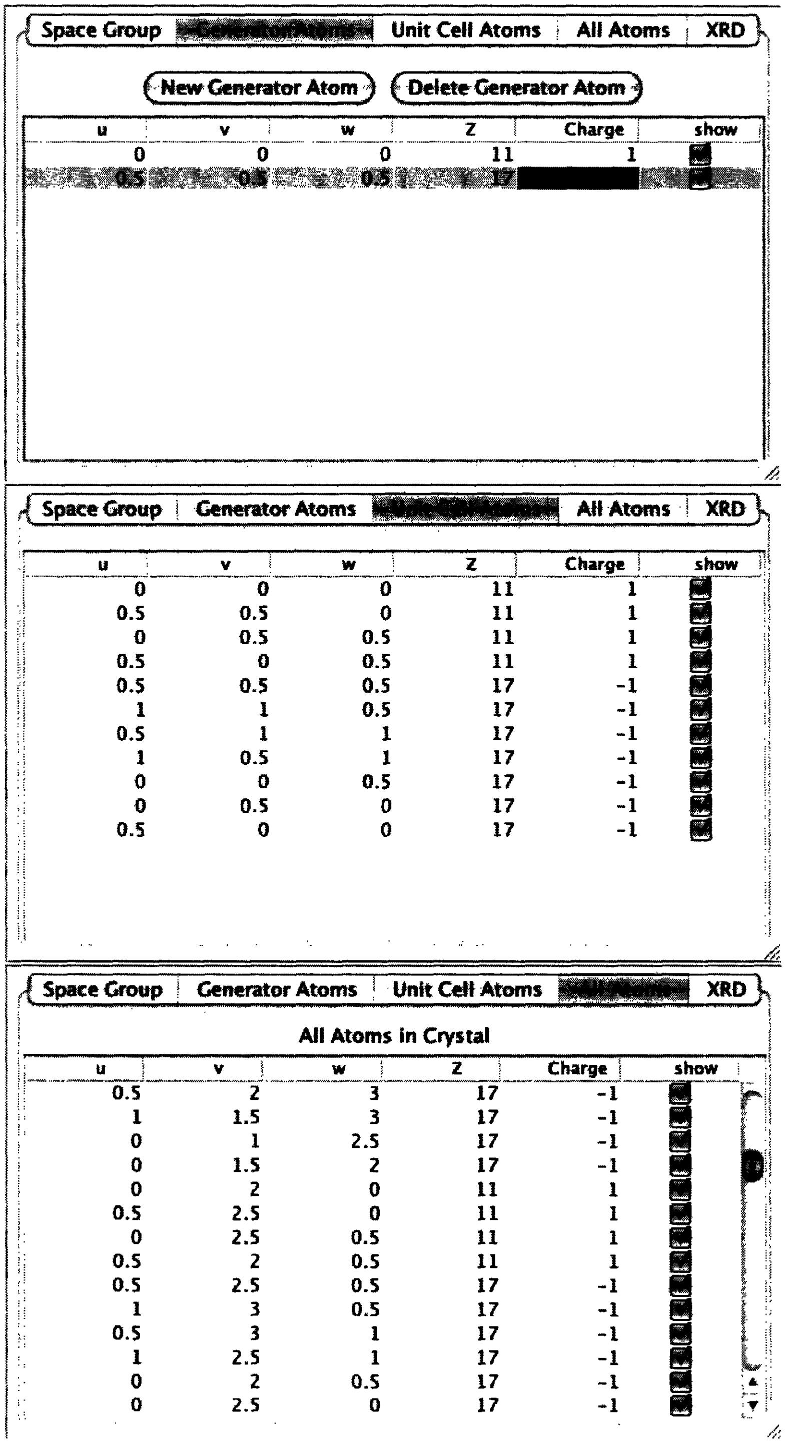
Space Group
Unit Cell Atoms
All Atoms
XRD
New Generator Atom
Delete Generator Atom

u	v	w	Z	Charge	show
0	0	0	11	1	☑
0.5	0.5	0.5	17		☑

Space Group
Generator Atoms
All Atoms
XRD

u	v	w	Z	Charge	show
0	0	0	11	1	☑
0.5	0.5	0	11	1	☑
0	0.5	0.5	11	1	☑
0.5	0	0.5	11	1	☑
0.5	0.5	0.5	17	-1	☑
1	1	0.5	17	-1	☑
0.5	1	1	17	-1	☑
1	0.5	1	17	-1	☑
0	0	0.5	17	-1	☑
0	0.5	0	17	-1	☑
0.5	0	0	17	-1	☑

Space Group
Generator Atoms
Unit Cell Atoms
XRD

All Atoms in Crystal

u	v	w	Z	Charge	show
0.5	2	3	17	-1	☑
1	1.5	3	17	-1	☑
0	1	2.5	17	-1	☑
0	1.5	2	17	-1	☑
0	2	0	11	1	☑
0.5	2.5	0	11	1	☑
0	2.5	0.5	11	1	☑
0.5	2	0.5	11	1	☑
0.5	2.5	0.5	17	-1	☑
1	3	0.5	17	-1	☑
0.5	3	1	17	-1	☑
1	2.5	1	17	-1	☑
0	2	0.5	17	-1	☑
0	2.5	0	17	-1	☑

Figure 6.2: The three atom list panels for the NaCl crystal structure.

interactively rotate the crystal. This allows the user to see the crystal from all angles and get a full sense of its 3D structure. Figure 6.3 shows some various visualizations the NaCl crystal structure.

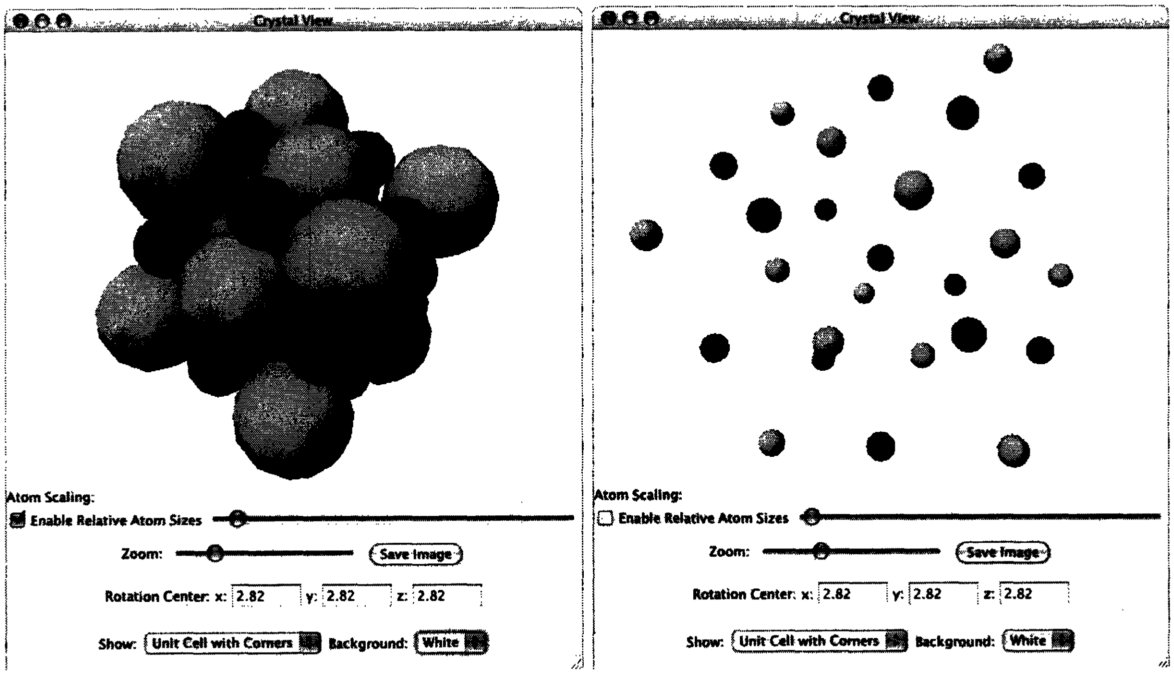

Atom Scaling:
☑ Enable Relative Atom Sizes
Rotation Center: x: 2.82 y: 2.82 z: 2.82
Show: Unit Cell with Corners Background: White

Atom Scaling:
☐ Enable Relative Atom Sizes
Rotation Center: x: 2.82 y: 2.82 z: 2.82
Show: Unit Cell with Corners Background: White

Figure 6.3: NaCl crystal visualization in AtomicControl.

6.4 Virtual diffractometer

Once the crystal is defined, the user needs only to go to the XRD panel and press the "Diffract" button to have AtomicControl calculate an x-ray powder diffraction pattern. In this panel, the user may also choose the x-ray target from a list of common target elements. When the "Diffract" button is pressed, the diffractometer windows appear. These windows provide a plot of the diffraction intensities plotted against 2θ. They also provide an interactive viewer of the reciprocal lattice of the crystal. In this view spheres with diameters that are proportional to structure factor at each reciprocal lattice vector allow the user to understand the concept of a reciprocal lattice and how it relates to the diffraction pattern. The diffractometer windows are shown in Fig. 6.4 with the example of NaCl.

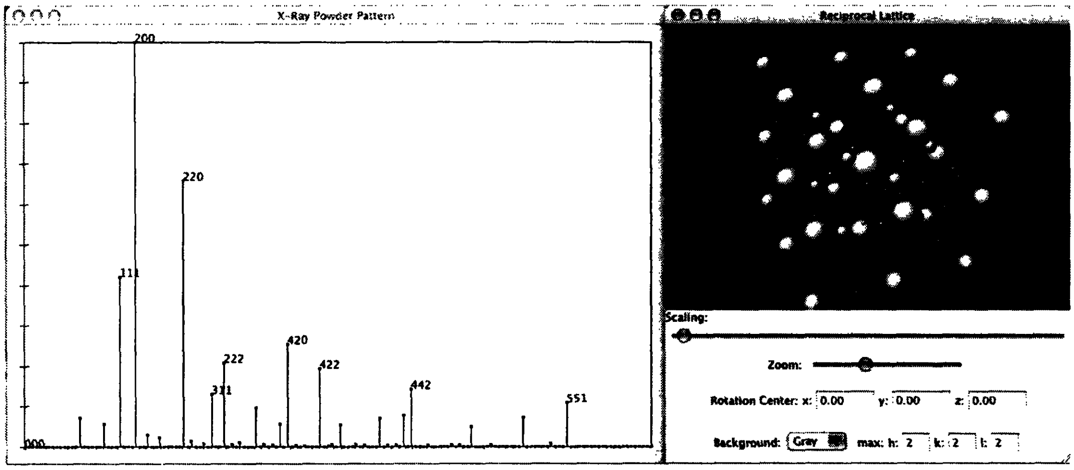
X-Ray Powder Pattern
Reciprocal Lattice
200
220
111
420
222
422
311
442
551
000
Scaling:
Zoom:

Rotation Center: x: 0.00 y: 0.00 z: 0.00

Background: Gray max: h: 2 k: 2 l: 2

Figure 6.4: X-ray diffraction pattern and reciprocal lattice viewer of NaCl produced by AtomicControl.

6.5 Saving and retrieving data

AtomicControl provides the capability to save the crystal data in an XML file format (see Chapter 2). The File menu, seen in Fig. 6.5, allows the user to save or open a file in this format. This menu will also allow the user to export the crystal view to an image file and save the x-ray diffraction pattern to a spreadsheet file.

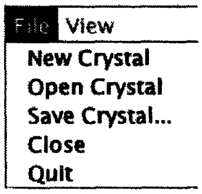
File
View
New Crystal
Open Crystal
Save Crystal...
Close
Quit

Figure 6.5: The File menu of AtomicControl.

Chapter 7

Lesson Plans

Since AtomicControl is intended to be used in the classroom, this section provides three examples that illustrate to the instructor or student how to use AtomicControl to observe and understand the relationship between structure and diffraction pattern. These examples can be combined with laboratory experiments that would allow the student to compare simulated data with experimental results.

7.1 Redefining the unit cell

The conventional unit cell of the body-centered cubic Bravais lattice is not a primitive unit cell. Each cube contains two lattice points within it: the corner point and the body-center point. It is possible to redefine the lattice using three non-orthogonal vectors that create a unit cell with only one lattice point. The choice between these two cell definitions should be arbitrary and one should be able to pick the definition that suits current needs.

However, on first observation of the mathematical definition of the structure formula, it appears that an x-ray diffraction pattern would be dependent on this rather arbitrary definition of the unit cell. This should not seem right, because the physics of diffraction should not change when the mathematical definition of the unit cell changes. In the end, both definitions produce the same crystal and therefore should produce the same diffraction pattern. This lesson plan shows how these two different lattice definitions may be visualized in AtomicControl and shows that the x-ray diffraction pattern does not change upon redefinition.

Conventional BCC

The standard space group definition of $Im\bar{3}m$ (no. 229) in AtomicControl provides the symmetry BCC iron. However, for the purpose of this lesson, a primitive cubic lattice will be used and atoms will be placed in the corner and body-centered positions to illustrate that the unit cell contains two lattice points. The lowest symmetry cubic lattice is $P23$ (no. 195) and will work well as a starting point for this structure. The lattice constant of BCC iron (α-Fe) is known to be $a = 2.8664\text{Å}$ [11]. Two generators atoms will need to be defined to make a BCC structure in a primitive cubic lattice. In the generator panel, create two iron atoms, one at the corner (0,0,0) and one at the body center $(\frac{1}{2}, \frac{1}{2}, \frac{1}{2})$. The space group panel for this structure is shown in Fig. 7.1 along with the resulting visualization.

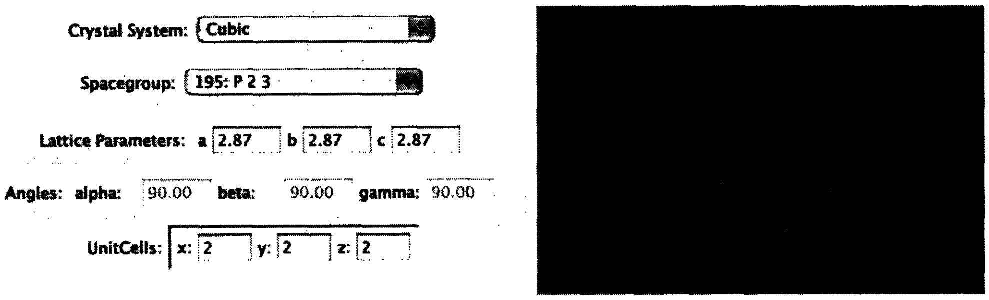

Crystal System: Cubic

Spacegroup: 195: P 2 3

Lattice Parameters: a 2.87 b 2.87 c 2.87

Angles: alpha: 90.00 beta: 90.00 gamma: 90.00

UnitCells: x: 2 y: 2 z: 2

Figure 7.1: Space group panel of conventional BCC iron and resulting unit cell.

From the definition of the two generator atoms, the structure factor for the convention cell of BCC iron is

$$F(\vec{G}) = \sum_{j=0}^{\text{unit cell}} f_j e^{i\vec{G}\cdot\vec{R}_j} = f_{\text{Fe}}(1 + e^{i\pi(h+k+l)}) \tag{7.1}$$

Primitive BCC

The primitive lattice of BCC can be defined by three vectors that connect the convention corner point to three non-coplanar body-center points as seen in Fig. 7.2. This creates a short bipyramidal unit cell that only contains one lattice point. These vectors can be defined in cartesian coordinates as

$$\vec{a_1} = \frac{a}{2}(-\hat{x} + \hat{y} + \hat{z}) \qquad \vec{a_2} = \frac{a}{2}(\hat{x} - \hat{y} + \hat{z}) \qquad \vec{a_3} = \frac{a}{2}(\hat{x} + \hat{y} - \hat{z}) \tag{7.2}$$

To create this lattice in AtomicControl, all symmetry is removed by picking the triclinic space group $P1$ (no. 1). AtomicControl allows the definition of the lattice vectors through the definition of lattice constants and interaxial angles in the space group panel. The magnitudes of $\vec{a_1}$, $\vec{a_2}$, and

$\vec{a_3}$ are all equal to $\frac{\sqrt{3}}{2}a = 2.4824\text{Å}$. The angle between any two of the vectors is the tetrahedral angle, 109.5^o. α, β, and γ are the angles between $\vec{a_2}$ and $\vec{a_3}$, $\vec{a_1}$ and $\vec{a_3}$, and $\vec{a_1}$ and $\vec{a_2}$, respectively.

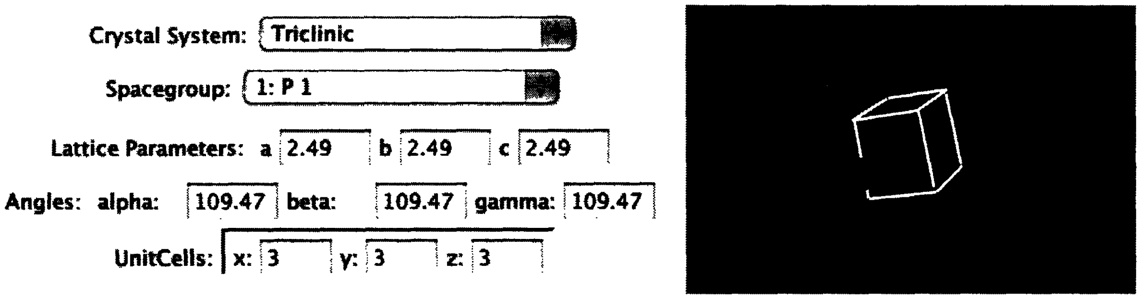
Crystal System: Triclinic
Spacegroup: 1: P 1
Lattice Parameters: a 2.49 b 2.49 c 2.49
Angles: alpha: 109.47 beta: 109.47 gamma: 109.47
UnitCells: x: 3 y: 3 z: 3

Figure 7.2: Space group panel of primitive BCC Fe and resulting crystal structure. The conventional unit cell is outlined.

The structure factor of the BCC structure defined in this primitive fashion is

$$F(\vec{G}) = \sum_{j}^{\text{unit cell}} f_j e^{i\vec{G}\cdot\vec{R_j}} = f_{\text{Fe}} e^{i2\pi\cdot 0} = f_{\text{Fe}}. \tag{7.3}$$

This definition looks much different than that of the conventional cell definition shown in Eq. 7.1.

Changes in definition do not change diffraction

Since the intensity of a diffraction peak is proportional to $|F|^2$ it would seem that the primitive definition would cause more peaks to be present than the conventional cell. while $F_{\text{primitive}}$ always equals f_{Fe}, $F_{\text{Conventional}}$ can go to zero at certain reciprocal lattice vectors and at their associated scattering angles. However, if you click the diffract button after creating both of these structures, the diffraction pattern will look the same.

The key difference between the two definitions is that they do not have the same reciprocal lattice vectors. In fact, the conventional unit cell has twice as many reciprocal lattice points. However these extra reciprocal lattice vectors do not produce additonal diffraction conditions because the structure factor of the conventional cell guarantees that the ones that do not line up with the primitive cell's reciprocal lattice vectors have their diffraction amplitude extinguished. All that has been done by redefining the unit cell is redefining how the atomic planes are designated. For example the (110) in the conventional cell is now designated the (100) in the primitive cell. The two identical diffraction patterns are shown in Fig. 7.1 with their respective naming schemes.

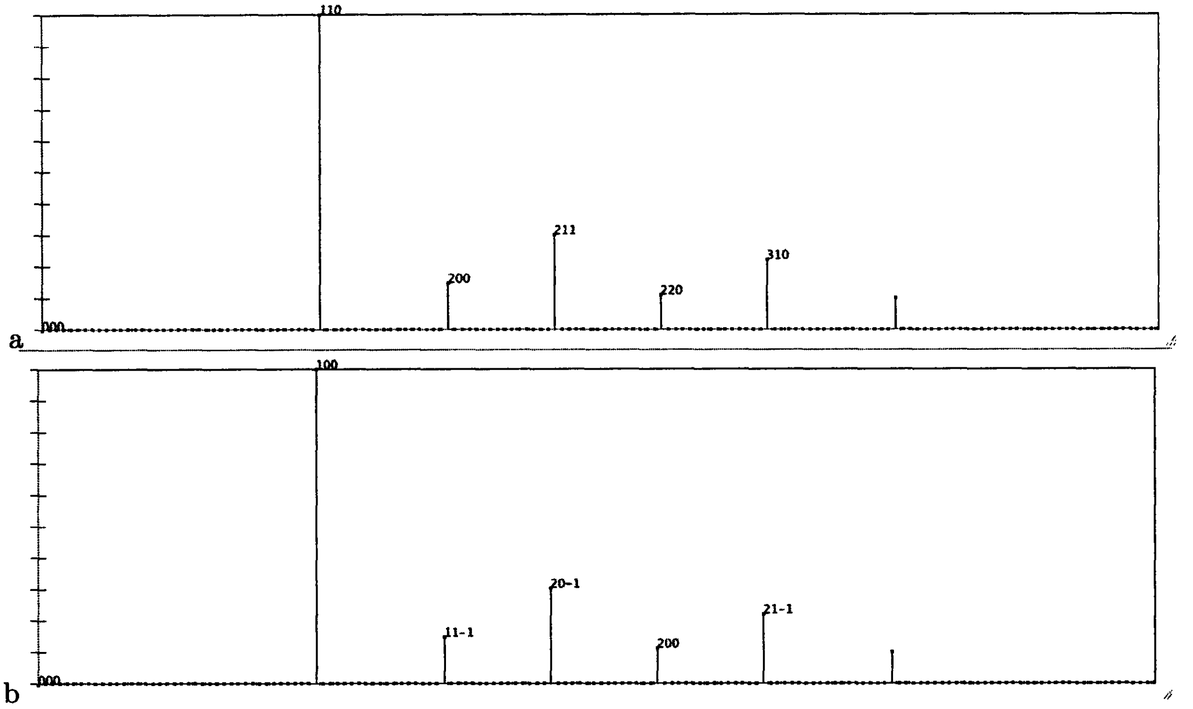

Figure 7.3: Simulated diffraction patterns of (a) conventional unit cell BCC and (b) primitive unit cell BCC. Only the *hkl* labels are different.

7.2 Cu_3Au order-disorder transformation

This lesson plan focuses on the change that occurs in the Cu_3Au order-disorder transformation and its resulting changes in x-ray diffraction pattern. Ordered Cu_3Au is has a primitive cubic structure with gold at the corners and copper in the face center positions. When Cu_3Au is quenched from high temperatures, it stays in a disordered state where both copper and gold will occupy both sites — corner and face-center — randomly. This gives this structure $Fm\bar{3}m$ symmetry and the atomic scattering factors will be a weighted average of the Au and Cu content in the alloy.

X-ray diffraction can be a useful tool in understanding the degree of ordering in such a system. The first step in understanding how structure effects the diffraction is to build the crystals in AtomicControl.

Building ordered Cu_3Au

Building a crystal in AtomicControl first requires definition of the crystal system and space group. This is done in the space group panel as seen in Fig. 7.4. Ordered Cu_3Au has a primitive cubic lattice. The first step is to select a cubic crystal system. The next step is to pick a space group;

ordered Cu_3Au has $Pm\bar{3}m$(no. 221) symmetry. The lattice constant has been determined to be $a = 3.7493$Å [12] and also can be entered in the space group panel.

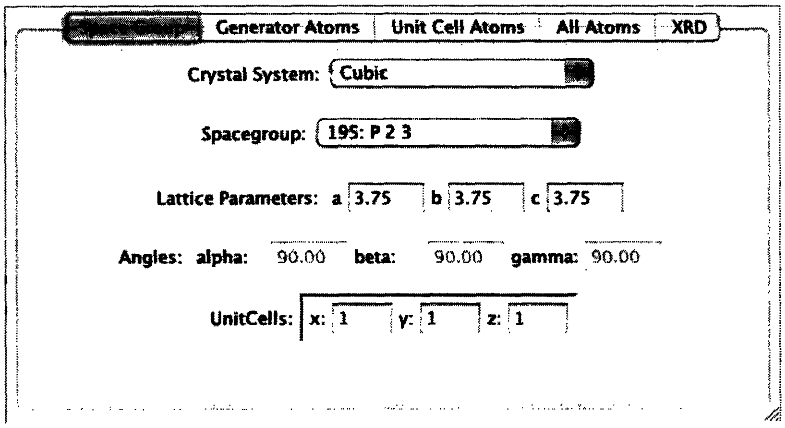

Crystal System: Cubic

Spacegroup: 195: P 2 3

Lattice Parameters: a 3.75 b 3.75 c 3.75

Angles: alpha: 90.00 beta: 90.00 gamma: 90.00

UnitCells: x: 1 y: 1 z: 1

Figure 7.4: Space group panel with Cu_3Au lattice parameters entered.

The next step is to define the atoms in the unit cell. The gold atoms will be at the corners of the unit cell with coordinates (0,0,0) and the copper atoms will be at the face-centers with coordinates $(\frac{1}{2}, \frac{1}{2}, 0)$. These can be added to the generator panel. There are three face-center atoms per unit cell, but it is only necessary to define one. The three-fold symmetry around the [111] direction required by the space group $Pm\bar{3}m$ will cause the others to be generated. It is possible to observe the generated unit cell by observing the crystal view seen in Fig. 7.2 as well as their fractional coordinates in the unit cell atoms panel.

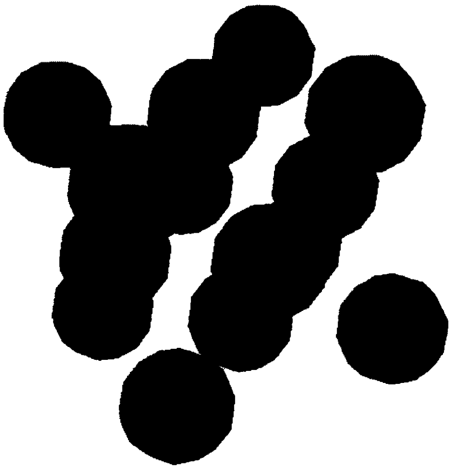

Figure 7.5: Ordered Cu_3Au visualization. Corner atoms are Au, face-centered atoms are Cu.

Building disordered Cu_3Au

Disordered Cu_3Au is FCC with each site having an average occupancy of 75% Cu and 25% Au. Therefore the diffraction pattern should look very similar to that of FCC copper. In order to build FCC copper, the space group must be defined in the space group panel as $Fm\bar{3}m$ (no. 225) and the lattice constant is $a = 3.6150$Å. The single generator atom is a Cu — really an average of Cu and Au — atom at (0,0,0) for this structure.

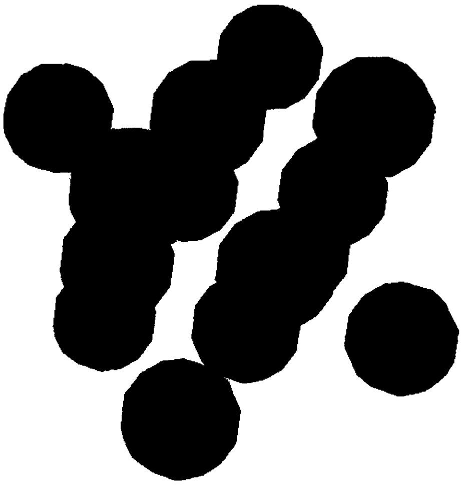

Figure 7.6: FCC copper unit cell visualization.

X-Ray diffraction comparison

The reduction in symmetry when the Cu_3Au is in its ordered state causes addition "superlattice" diffraction peaks to be visible, as seen in Fig. 7.7. For example, the the 100 and 110 peaks are not visible in an FCC structure, but appear in a primitive cubic structure.

In this lesson the extremal conditions of perfect order and complete disorder were investigated. Real crystals will never be fully ordered or disordered, so experimental data will lie between these two extremes. However, understanding the diffraction pattern of the limiting cases is useful because a sample that is partially ordered will exhibit aspects of both and makes it possible to use the powder-pattern to determine the order parameter of the system.

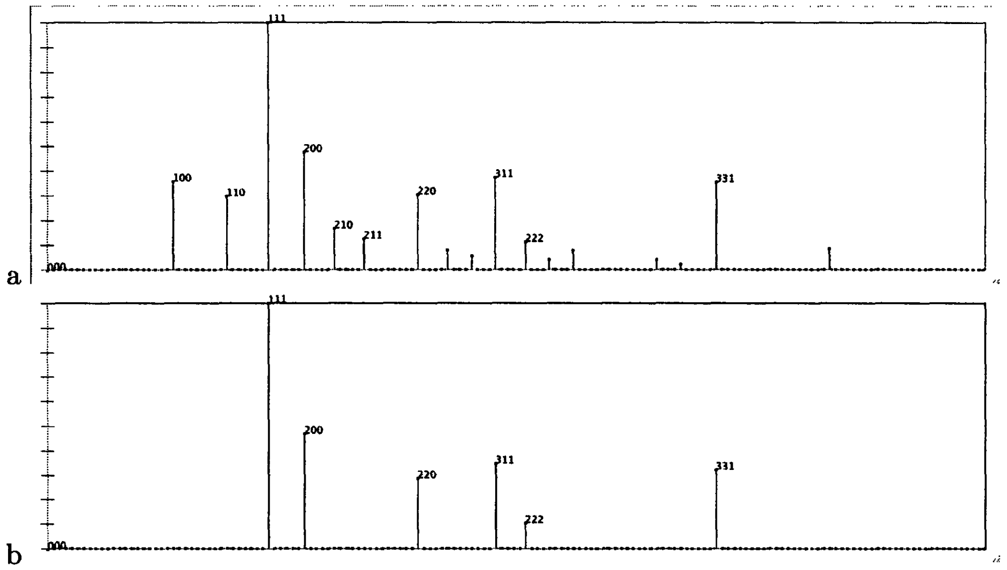

Figure 7.7: Comparison of x-ray powder diffraction patterns of (a) ordered and (b) disordered Cu_3Au . Note that (b) is FCC and only *hkl* unmixed are visible, while (a) is primitive cubic and all *hkl* appear.

7.3 Cubic-to-tetragonal transition

The expansion or compression of a cubic lattice along a single four-fold symmetry axis causes a transition to tetragonal symmetry. When this expansion or compression occurs it produces additional interplanar spacings that were not present in the cubic phase, and thus changes the x-ray diffraction pattern. This type of transition occurs in many systems, but is most well-known in the martensitic transformation of steel.

In pure iron, the high temperature to low temperature transition leads to the conversion from FCC austenite to BCC ferrite. When carbon is added to the system, a transition to tetragonal martensite occurs as carbon atoms get stuck in interstitial sites during rapid quenching. This transition in steel consists of a compression of the FCC unit cell in the [001] direction. This leads to a shortened tetragonal lattice which appears to be face-centered, but by convention is referred to an equivalent body-centered tetragonal Bravais lattice. This lesson provides a comparison of x-ray diffraction between FCC austenite and these two definitions of tetragonal martensite.

Building austenite

Austenite is the term used for high temperature FCC phase of iron (γ-Fe) in the Fe-C steel system. The space group of austenite is $Fm\bar{3}m$, but in this lesson it will be defined as a special case of the tetragonal space group $P4/mmm$ (no. 123). Since this is actually a cubic crystal, the lattice constants must be set equal in the space group panel $a = b = c = 3.6065$Å [13] as seen in Fig 7.8. The resulting x-ray diffraction pattern is shown in Fig. 7.12a. Three generator atoms are required to create the face-centered structure on the primitive tetragonal lattice. (0,0,0) generates the corner atoms, $(\frac{1}{2}, \frac{1}{2}, 0)$ generates the tetragonal axis face-center atoms, and $(0, \frac{1}{2}, \frac{1}{2})$ generates the remaining of the face-center atoms.

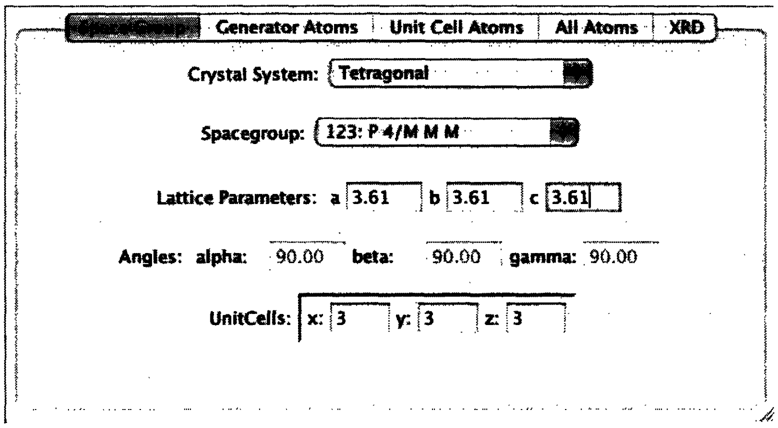

Crystal System: Tetragonal

Spacegroup: 123: P 4/M M M

Lattice Parameters: a 3.61 b 3.61 c 3.61

Angles: alpha: 90.00 beta: 90.00 gamma: 90.00

UnitCells: x: 3 y: 3 z: 3

Figure 7.8: Space group panel definition of austenite.

Building martensite

Martensite structure is a result of the non-equilibrium compression of the c-axis in FCC austenite. Taking the crystal structure of austenite that was just created, it is simple to apply this compression by decreasing the lattice constant c by a small percentage in the space group panel as seen in Fig. 7.9. (By convention the tetragonal axis is in the c direction.) This is not the conventional unit cell definition of martensite, but it illustrates peak splitting without redefinition of hkl values. The resulting x-ray diffraction pattern is shown in Fig. 7.12b.

Redefining martensite

The martensite structure is conventionally defined on a body-centered tetragonal Bravais lattice. The deformed face-centered structure is that was just created is compared with this BCT lattice in Fig. 7.10. This geometry leads to a $I4/mmm$ symmetry and lattice constants $a' = b' = \frac{\sqrt{2}}{2}a$ and $c' = c$ as seen in the space group panel in Fig. 7.11.

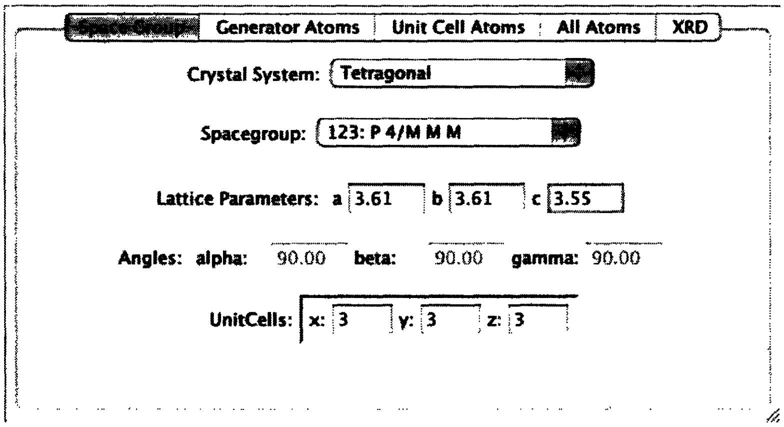
Space Group
Generator Atoms
Unit Cell Atoms
All Atoms
XRD

Crystal System: Tetragonal

Spacegroup: 123: P 4/M M M

Lattice Parameters: a 3.61 b 3.61 c 3.55

Angles: alpha: 90.00 beta: 90.00 gamma: 90.00

UnitCells: x: 3 y: 3 z: 3

Figure 7.9: Space group panel definition of martensite.

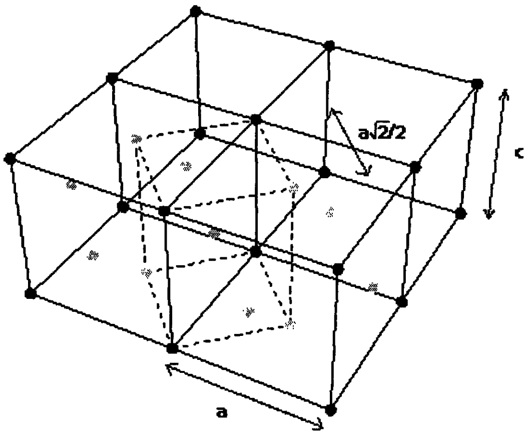

Figure 7.10: The geometric relationship between the compressed face-centered structure to the body-centered tetragonal (BCT) lattice. Dotted lines outline the BCT unit cell [14].

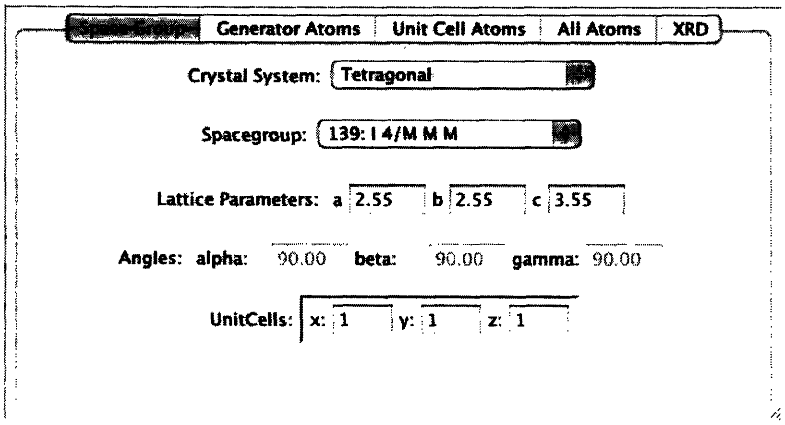
Space Group
Generator Atoms
Unit Cell Atoms
All Atoms
XRD

Crystal System: Tetragonal

Spacegroup: 139: I 4/M M M

Lattice Parameters: a 2.55 b 2.55 c 3.55

Angles: alpha: 90.00 beta: 90.00 gamma: 90.00

UnitCells: x: 1 y: 1 z: 1

Figure 7.11: Space group panel definition of BCT martensite.

X-ray diffraction comparison

In austenite, the cubic symmetry makes {200} family planes have the same spacing and therefore the same diffraction angle. The tetragonal martensite phase (defined as face-centered), however, has the same lattice spacing for (200) and (020) but not in for (002). This has the effect of splitting the {200} family peak to form one peak from scattering on (200) and (020) planes, and a separate peak from scattering on (002) planes. This peak splitting can be seen by comparing the calculated x-ray diffraction patterns in Figures 7.12a and 7.12b. Using the conventional BCT definition of martensite, the x-ray diffraction pattern will not change, but the designation of *hkl* values will, as seen in the comparison between Figures 7.12b and 7.12c.

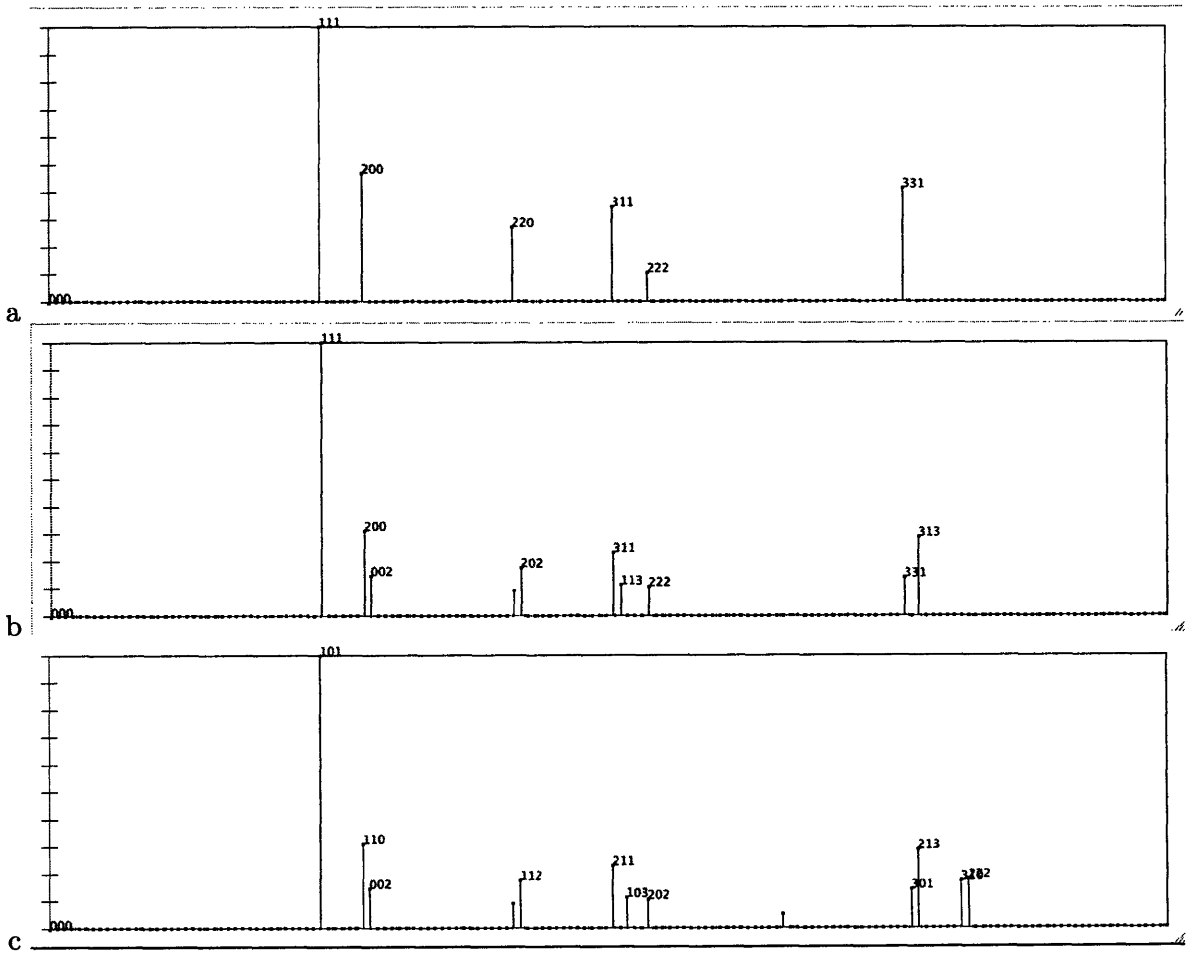

Figure 7.12: (a) Austenite (FCC) x-ray diffraction pattern. (b) Martensite (face-centered definition) x-ray diffraction pattern. (c) Martensite (BCT) x-ray diffraction pattern. Note the splitting of the (200) peak from (a) to (b). (b) and (c) are identical except for the designation of *hkl* values.

Chapter 8

Conclusions

AtomicControl was designed to fit a specific need of replacing Cerius^2 in the MIT classroom. It succeeds in making building a crystal a user-friendly process. The hope is that it will be adopted as a teaching tool by the instructors of the new crystallography and diffraction subjects in 3.012 and 3.014. No software is complete and AtomicControl is not an exception. AtomicControl still needs to be tested more fully with more complex crystal structures and its graphic user interface could be improved. The modular object-oriented design of AtomicControl makes it easy to be extended and modified. The source code of AtomicControl will be released to the public under a public license so that others can modify AtomicControl to fit their needs. The hope is that AtomicControl will become useful to the materials science community at large.

Bibliography

[1] MIT. Report of the Athena/SGI Strategy Discovery Project, January 2000. URL `http://web.mit.edu/cease/www/report.html`.

[2] Sun Microsystems. Java Technology, 2005. URL `http://java.sun.com`.

[3] World Wide Web Consortium. Extensible Markup Language (XML), April 2005. URL `http://www.w3.org/XML/`.

[4] S. M. Allen and E. L. Thomas. *The Structure of Materials.* Wiley, New York, 1999.

[5] T. Hahn, editor. *International Tables for Crystallography*, volume A: Space Group Symmetry. Springer, 5th edition, March 2002.

[6] V. L. Himes and A. D. Mighell. A Matrix Approach to Symmetry. *Acta Crystallographica Section A*, 43(3):375–384, May 1987.

[7] B. Rupp. Macromolecular Crystallography Web Site, December 2004. URL `http://www-structure.llnl.gov/`.

[8] E. W. Weisstein. MathWorld: Fraunhofer Diffraction, 2005. URL `http://scienceworld.wolfram.com/physics/FraunhoferDiffraction.html`.

[9] A. Guinier. *X-Ray Diffraction.* W. H. Freeman and Company, San Francisco, 1963.

[10] B. D. Cullity and S. R. Stock. *Elements of X-Ray Diffraction.* Prentice-Hall, Inc., third edition, 2001.

[11] H. E. Swanson et. al. *Standard X-ray Diffraction Patterns.* National Bureau of Standards, Washington, DC, 1953-62.

[12] Materials Data Incorporated. *Jade Software Database.* Livermore, CA, 2005. URL `http://www.materialsdata.com/`.

[13] A. M. Streicher-Clarke, J. G. Speer, D. K. Matlock, B. C. Decooman, and D. L. Williamson. Analysis of Lattice Parameter Changes Following Deformation of a 0.19C-1.63Si-1.59Mn Transformation Induced Plasticity Sheet Steel. *Metallurgical and Materials Transactions A*, 36(4): 907–918(12), April 2005.

[14] K. F. Hane. Microstructures in thermoelastic martensitic transformations, 1998. URL `http://www.aem.umn.edu/people/faculty/shield/hane/`.